Synthesis and Characterization of Single Crystal α-Fe_2O_3 Nanobelts

Hongzhe Wang, Xingtang Zhang, Bing Liu, Huiling Zhao, Yuncai Li, Yabin Huang, and Zuliang Du*
Key Laboratory for special Functional Materials, Henan University, Kaifeng 475001, P. R. China

(Received October 28, 2004; CL-041276)

Single crystal nanobelts of hematite (α-Fe_2O_3) with narrow width distribution centered at 230 nm and length up to several microns have been prepared in NaCl flux using a simple solid-state reaction. Characterizations show that the as-prepared nanobelts are single-crystalline.

Recently, preparation of well-defined quasi-one-dimensional solid nanostructures, nanowires, and nanobelts has stimulated considerable interest for scientific research because of their importance in mesoscopic physics studies and their potential applications. Many methods have been devised to synthesize 1D nano-sized materials, such as arc discharge,[1] templating,[2] and others.[3–5] Wang and co-workers[6–8] have synthesized metal oxide nanobelts of ZnO and SnO_2, and field-effect transistors have been fabricated using individual nanobelt.[9]

Among all metal oxides, iron oxides are extensively studied for catalysis[10,11] and magnetic storage. Hematite with morphologies of spindle, rod, and sphere has been synthesized through hydrolysis and aging of ion(II) salts using methods adopted or adjusted from Matijević et al.[12] and Ozaki et al.[13] To our knowledge, no belt-like α-Fe_2O_3 has been reported.

The process of solid-state reaction, recognized as a simple and effective technique has achieved many fascinating results in preparing nanomaterials. Nanoparticles and nanorods had been successfully synthesized using this method.[14,15] Wang et al. had reported the preparation of single crystal Mn_3O_4 nanowires using surfactant and salt-flux-aided solid-state reaction.[16] Herein, we report the synthesis of single crystal α-Fe_2O_3 nanobelts using a simple approach similar to that developed by Wang et al. in ref 16 that exploits a solid-state reaction to prepare nanometer-sized precursors and subsequently forming α-Fe_2O_3 nanobelts in NaCl flux. In a typical synthesis, 3.25 g of $FeCl_3 \cdot 6H_2O$ and 3.18 g of Na_2CO_3 were mixed in 50 mL of distilled water, stirred moderately for complete reaction. The product was filtered and dried in an oven at 60 °C for 3 h. The obtained product (0.4 g) was mixed with NaCl (1.5 g) and 2 mL span-80 (Sorbitan Monooleate) in an agate mortar and ground for 20 min, and then heated in a porcelain crucible at 830 °C for 2.5 h. At last, the heat-treated sample was cooled gradually to room temperature in air, washed several times with distilled water, filtered and dried to obtain powder sample with bright red hue. The as-prepared powder sample was characterized by X-ray diffraction (XRD) (Philips, X' Pert Pro MPD), X-ray photoelectron spectroscopy (XPS) (KRATOS Analytical Ltd., Axis ultra), and transmission electron microscopy (TEM) (JEOL, 100CXII at 100kV).

Figure 1a shows the XRD pattern of the as-prepared sample. The XRD spectrum indicates that the final product is highly crystallized α-Fe_2O_3 and almost all the peaks can be indexed to the hexagonal structure of hematite except the one at 30 degree, which may be caused by another phase of Fe_2O_3 produced under high-temperature treatment.

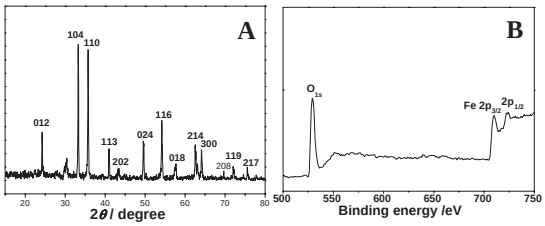

Figure 1. (A) XRD pattern of the as-prepared sample. (B) XPS spectrum of the obtained sample.

Element valences in the sample were determined by XPS. The C1s binding energy of 284.8 eV was accepted as a standard. Figure 1b exhibits the result of XPS analysis. The appearance of a characteristic Fe $^2p_{1/2}$ peak at 724.5 eV, Fe $^2p_{3/2}$ peak at 710.9 eV, and O_{1s} peak at 531.0 eV confirms the abundant existence of Fe_2O_3 in the sample. The XPS spectrum proved that there was no Fe_3O_4 existing but only a little amount of other phase of Fe_2O_3 presented in the sample as byproduct and this also validated our speculation in XRD study.

The morphology of as-prepared sample was characterized by TEM. Typical TEM images shown in Figure 2 displayed the morphology of representative α-Fe_2O_3 nanobelts prepared in this method. From Figures 2a and 2b we can see clearly that the nanobelts are very smooth with narrow width distribution centered at 230 nm and length up to several microns. We also find some shorter ones in Figure 2b, which may be the rudiments of the nanobelts or broken ones destroyed by high temperature. Nanobelts grew along the edge of micrometer-sized Fe_2O_3 particles and this phenomenon might be caused by specific active facets produced in the grinding process distributed on the particle surface and those active facets acted as preferred initial growth bases for the formation of nanobelts under following annealing treatment. Figure 2c shows a typical single nanobelt, we can see clearly that there are no spherical particles on the top, which can be taken as evidence for vapor–liquid–solid (VLS)[17] growth mechanism. Photograph of TEM in Figure 2d shows the high-resolution transmission electron microscopy (HRTEM) image corresponding to the boxed area in Figure

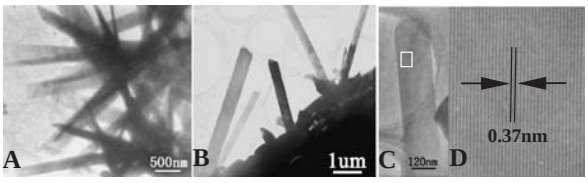

Figure 2. (A) and (B) Low-magnification TEM images of the α-Fe_2O_3 nanobelts. (C) A typical single nanobelts and (D) High-resolution TEM image of the boxed area in Figure 2C.

2c. The clear lattice fringes reveal that the α-Fe_2O_3 nanobelt is a structurally uniform single crystal without dislocation. The spacing of 0.37 nm between adjacent lattice planes corresponds to two (012) crystal planes of α-Fe_2O_3, which indicates that the direction perpendicular to [012] is the preferred growth direction for the single-crystalline nanobelts.

In the synthesis process, span-80 was used as dispersive solvent and surfactant for the formation of fine particles when the reactants were ground. The carbonization of span-80 under high temperature decreases the eutectic temperature of the mixed system.[18] Melten NaCl decreased the viscosity of reactant system when the temperature was raised up to 830 °C, while the melting point of NaCl is about 801 °C.[16,18] It prevented those fine particles from aggregation by capping them[19] and aided the conglomeration of fine particles towards those active sites distributed on the micrometer-sized particles. Those active sites captured the fine particles dispersed among the NaCl flux, inducing the crystallization of α-Fe_2O_3 particles at these sites and basal protuberances presented. Then, the rudiments of nanobelts formed in a short period of time. As more and more fine particles were transported towards those bases by the flux, rudiments kept growing longer and longer with continuously crystallization of the newcomers and zonary α-Fe_2O_3 nanobelts were finally formed. The width of nanobelts may be determined by the size of the initial active sites.

To summarize, we have successfully synthesized α-Fe_2O_3 nanobelts using a simple method. Structural features and chemical compositions of the as-prepared sample were investigated using XRD, TEM, and XPS. The characterization of the product indicated that the as-synthesized α-Fe_2O_3 nanobelts are smooth, uniform and highly crystalline.

This work was supported by Natural Science Foundation of China (No. 90306010 and 20371015) and State Key Basic Research “973” Plan of China (No. 2002CCC02700).

References

1 S. Iijima, *Nature*, **354**, 56 (1991).
2 C. R. Martin, *Science*, **266**, 1961 (1994).
3 W. S. Shi, Y. F. Zheng, N. Wang, C. S. Lee, and S. T. Lee, *Adv. Mater.*, **13**, 591 (2001).
4 Z. W. Pan, Z. Dai, and Z. L. Wang, *Science*, **291**, 1947 (2001).
5 S. W. Liu, J. Yue, and A. Gedanken, *Adv. Mater.*, **13**, 656 (2001).
6 Z. R. Dai, Z. W. Pan, and Z. L. Wang, *Solid State Commun.*, **118**, 351 (2001).
7 Z. W. Pan, Z. R. Dai, and Z. L. Wang, *Appl. Phys. Lett.*, **80**, 309 (2002).
8 Y. Ding, P. X. Gao, and Z. L. Wang, *J. Am. Chem. Soc.*, **126**, 2066 (2004).
9 M. S. Arnold, P. Avouris, Z. W. Pan, and Z. L. Wang, *J. Phys. Chem. B*, **107**, 659 (2003).
10 R. Pestman, R. M. Koster, E. Boellaard, A. M. Van der Kraan, and V. Ponec, *J. Catal.*, **174**, 142 (1998).
11 S. S. Lin and M. D. Gurol, *Environ. Sci. Technol.*, **32**, 1417 (1998).
12 E. Matijević and P. Scheiner, *J. Colloid Interface Sci.*, **63**, 509 (1978).
13 M. Ozaki, S. Kratohvil, and E. Matijevic, *J. Colloid Interface Sci.*, **102**, 146 (1984).
14 F. Li, J. Xu, X. Yu, L. Chen, J. Zhu, Z. Yang, and X. Xin, *Sens. Actuators, B*, **81**, 165 (2002).
15 W. Wang, Y. Zhang, and G. Wang, *Chem. Commun.*, **2001**, 727.
16 W. Wang, C. Xu, G. Wang, Y. Liu, and C. Zheng, *Adv. Mater.*, **14**, 837 (2002).
17 Z. Wang, *J. Phys.: Condens. Matter*, **16**, R829 (2004).
18 Y. J. Chen, J. B. Li, Q. M. Wei, and H. Z. Zhai, *J. Cryst. Growth*, **224**, 244 (2001).
19 J. B. Wiley and R. B. Kaner, *Science*, **255**, 1093 (1992).

Published on the web (Advance View) January 15, 2005; DOI 10.1246/cl.2005.184